JTTEE5 3:282-288

Microstructure and Properties of Plasma-Sprayed Mo-Mo_2C Composites

S. Sampath and S.F. Wayne

Thermally sprayed molybdenum coatings are used in a variety of industrial applications, such as automotive piston rings, aeroturbine engines, and paper and plastics processing machinery. Molybdenum exhibits excellent scuffing resistance under sliding contact conditions. However, plasma-sprayed molybdenum coatings are relatively soft and require dispersion strengthening (e.g., Mo_2C) or addition of a second phase (e.g., NiCrBSi) to improve hardness, wear resistance, and thus coating performance. In this study, Mo-Mo_2C composite powders were plasma sprayed onto mild steel substrates. Considerable decarburization was observed during air plasma spraying—a beneficial condition because carbon acts as a sacrificial getter for the oxygen, thereby reducing the oxide content in the coating. Finer powders showed a greater degree of decarburization due to the increased surface area; however, the starting carbide content in the powder exerted very little influence on the extent of decarburization. The friction properties of Mo-Mo_2C coatings were significantly improved compared to those of pure molybdenum under continuous sliding contact conditions. It also was found that the abrasion resistance of the coatings improved with increasing carbide addition.

1. Introduction

MOLYBDENUM and molybdenum-base alloys are used extensively in a variety of engineering applications, particularly at high temperatures (>800 °C) (Ref 1). Molybdenum has a high melting point (2800 °C), combined with high thermal and electrical conductivity, low thermal expansion coefficient, and good high-temperature creep properties (Ref 2). However, molybdenum has low hardness and forms a low-melting-point and highly volatile oxide, both of which restrict applicability. Carbide-dispersion-strengthened molybdenum has significantly improved mechanical properties compared to unalloyed molybdenum, particularly at high temperatures (Ref 3). Typical carbide-dispersion-strengthened alloys include Ti-Zr-C-Mo (TZM) and HfC-Mo (HCM). Recently, Liao et al. (Ref 4) demonstrated improvement in molybdenum-matrix hardness through additions of Mo_2C, with implications for superior performance.

Key Words: carbon content, composite powders, molybdenum coatings, process dependency, wear behavior

S. Sampath, Osram Sylvania Inc., Chemical and Metallurgical Products, Towanda, PA 18848, USA (presently at Thermal Spray Laboratory, Department of Materials Science and Engineering, State University of New York, Stony Brook, NY 11794-2275, USA); and **S.F. Wayne**, Advanced Technology Center, Valenite Inc., Madison Heights, MI, USA.

Because of their unique tribological characteristics, thermally sprayed molybdenum coatings are used for automotive, aerospace, pulp and paper, and plastic processing applications. Molybdenum coatings are known to provide low friction and excellent resistance to scuffing under sliding contact conditions (Ref 5). The beneficial frictional behavior of molybdenum-base coatings has been identified by Overs et al. (Ref 6), who attribute the lowered friction to the formation of a surface film on molyb-

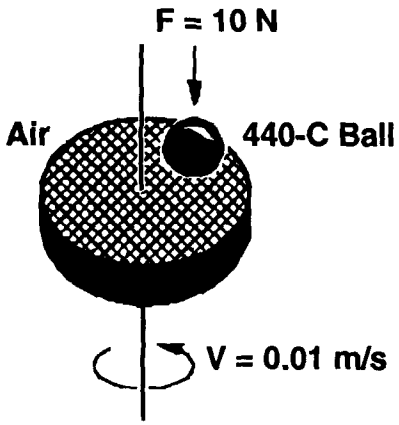

Fig. 1 Schematic of ball-on-disk friction and wear tester

Table 1 Powder characteristics

Powder	Composition(a)	Carbon, %	Oxygen, %	Particle size, μm
Molybdenum	Mo	...	0.1	−75 +30
Composite 1	Mo-15Mo_2C	0.93	0.21	−75 +30
Composite 2	Mo-35Mo_2C	2.2	0.12	−75 +30
Composite 2C	Mo-35Mo_2C	2.26	0.11	−90 +45
Composite 3	Mo-55Mo_2C	3.17	0.05	−75 +30

(a) From quantitative x-ray diffraction analysis using standards (in volume percent)

denum. In the automotive industry, flame-sprayed molybdenum wire coatings are widely used as running surfaces on piston rings in internal combustion engines. These flame-sprayed coatings possess high hardness due to the formation of MoO_2, which acts as a dispersion hardener.

Plasma-sprayed molybdenum coatings are relatively soft (<300 HV) and do not possess adequate breakout and wear resistance (Ref 7). They are typically combined with wear-resistant self-fluxing alloys or MoO_2 to improve overall wear properties. However, such additions adversely affect friction characteristics due to nonuniform properties of the different lamellae in the coating (Ref 7). In the present study, Mo-Mo_2C composite powders with varying fractions of carbide were plasma sprayed in order to study the influence of particle size, starting chemistry, and processing conditions on decarburization. The effects of these microstructural changes on hardness, friction, and abrasion properties of the coatings also were investigated.

2. Materials and Methods

Molybdenum and three types of Mo-Mo_2C composite powders were examined. The Mo-Mo_2C composite powders (Composites 2 and 3) were produced by a patented manufacturing process described elsewhere (Ref 8). The powder characteristics are given in Table 1. Additionally, a coarser version of the Composite 2 powder, referred to as Composite 2C, was examined to determine the effects of particle size on coating structure.

The powders were plasma sprayed onto degreased and grit-blasted mild steel substrates to a thickness of 0.4 to 0.6 mm. The spray parameters are given in Table 2. Additionally, Plazjet and low-pressure plasma-sprayed (LPPS) coatings of Composite 3 powder were obtained from Nippon Steel Hardfacing. The spray parameters for these coatings are not available for this paper. The coatings were characterized using x-ray diffraction (XRD) and scanning electron microscopy (SEM). The Mo_2C contents

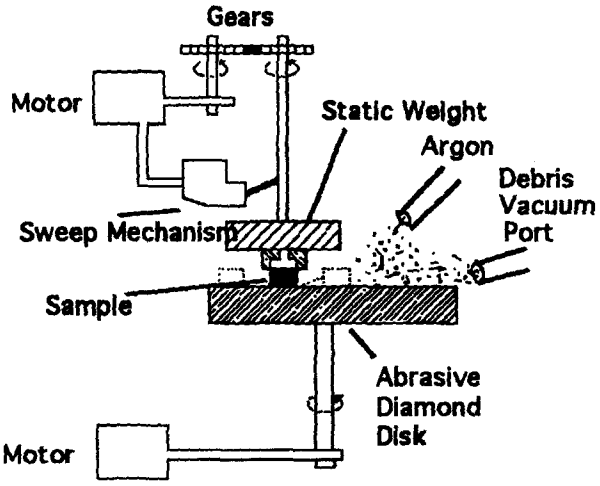

Fig. 2 Schematic of diamond abrasive wear tester

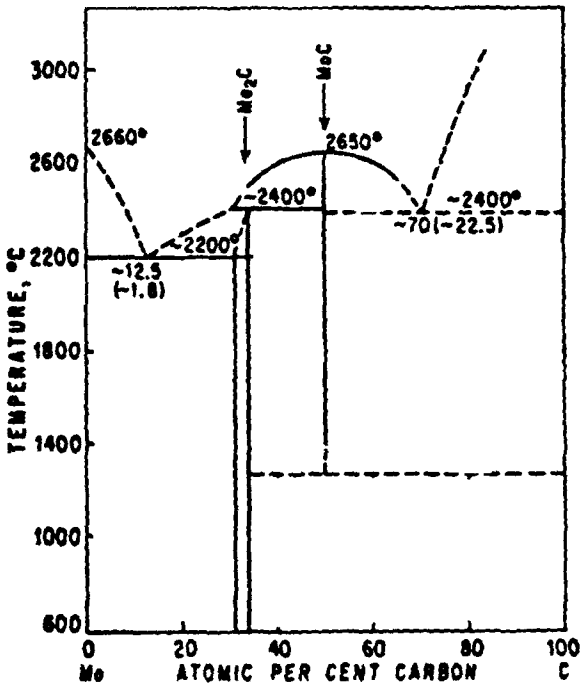

Fig. 3 Molybdenum-carbon phase diagram. Source: Ref 10

Table 2 Plasma spray parameters

Parameter	Description/unit
Gun	Metco 9MB
Nozzle	732
Current	500 A
Voltage	68 V
Argon flow	80(a)
Hydrogen flow	15(a)
Carrier argon	37(a)
Powder port	#2
Feed rate	30 g/min
Spray distance	10 cm

(a) Metco console units

Table 3 Coating characteristics

Powder	Process	Immersion density, cm^3	Carbon, wt%	Mo_2C, wt%	Carbon loss (from powder), wt%	Oxygen, wt%	Macrohardness, HRC	Microhardness, HV
Molybdenum	APS	9.36	...	...	...	1.1	21	295
Composite 1	APS	9.28	0.31	4	67	0.54	27	365
Composite 2	APS	9.05	0.81	9	69	0.51	28	382
Composite 2C	APS	9.13	0.69	7	63	0.41	28	385
Composite 3	APS	9.28	1.1	8	65	0.45	32	448
	Plazjet	...	1.23	21	61	...	42	700
	LPPS	...	3.1	55	0	...	58	1200

were obtained from quantitative XRD analysis using standards. In addition, coatings were separated from their substrates in order to measure total carbon and oxygen contents. Superficial hardness measurements on the coating surfaces were performed using a Rockwell 15N Brale indentor. Microhardness measurements were performed on coating cross sections using a diamond pyramid hardness tester at a load of 300 gf.

Friction and wear tests were performed using a ball-on-disk configuration and procedures established in the VAMAS program (Ref 9). Kinetic friction coefficients were measured in the unlubricated condition using a ball-on-disk configuration, as shown in Fig. 1. The plasma-sprayed coatings were metallographically polished through 600 grit (SiC) to achieve flat surfaces of uniform roughness prior to wear testing. The nominal thickness of the coatings after surface polishing was approximately 400 μm. The unidirectional sliding wear tests and friction measurements were carried out in air with a stationary AISI 440-C steel ball (9.5 mm diameter) mated against the rotating plasma-coated disk, producing a 10 mm wear-track diameter. The steel ball had a minimum hardness of 58 HRC and surface roughness of 0.038 μm.

The abrasive wear testing apparatus was the basic block-on-disk type, in which the disk was a removable, resin-bonded 45 μm diamond surface. The plasma-sprayed specimen was the block material. The block surface had a square geometry (1.25 by 1.25 cm) that was swept and rotated (20 rev/min) against the spinning (40 rev/min) abrasive disk. The apparatus is shown schematically in Fig. 2. The specimens were abraded for 1 min intervals, ultrasonically cleaned, hot-air dried, and subsequently weighed to a precision of 0.0001 g. All the specimens were abraded for a total time of 5 min. The density of the coatings was determined by first separating the coating from the substrate and then using the water-displacement method. The volume loss, and hence the abrasion rate, was calculated from the measured weight loss and density.

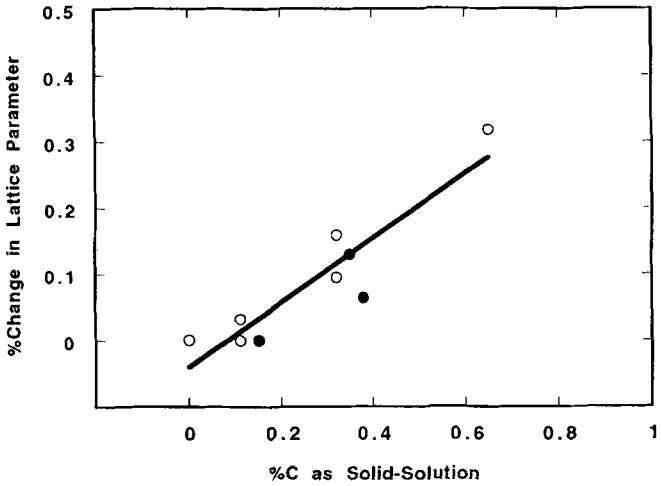

Fig. 4 Extended solid-solubility effects in plasma-sprayed Mo-Mo_2C coatings. The shaded data points are not included in Table 4.

3. Results and Discussion

Figure 3 shows the phase diagram of the molybdenum-carbon binary system (Ref 10). Solid solubility of carbon in molybdenum is limited to less than 0.018%, but it has been suggested that the solubility can be higher at temperatures above 1600 °C (Ref 10). As seen from the phase diagram, in the range of 0 to 6 wt% C, molybdenum and Mo_2C are produced from a eutectic reaction and coexist as stable phases below the eutectic temperature. The maximum carbon content in this study is 3.17 wt%, which corresponds to Mo-55 vol% Mo_2C (Table 1). X-ray diffraction studies and lattice parameter measurements suggest that all the carbon in the powder is accounted for as Mo_2C and do not indicate any free carbon or carbon dissolved in molybdenum in the powder.

3.1 *Decomposition Reactions during Spraying*

Carbide compounds partially decompose during atmospheric plasma spraying, following the reaction

$$2MC + \tfrac{1}{2} O_2 = M_2C + CO \quad \text{(Eq 1)}$$

and further

$$M_2C + \tfrac{1}{2} O_2 = 2M + CO \quad \text{(Eq 2)}$$

where MC and M_2C refers to the metal carbide (MoC and Mo_2C, respectively, in this case). This type of decomposition reaction was observed upon plasma spraying of Mo-Mo_2C composites (Eq 2 only). Table 3 compares the total carbon and Mo_2C present in the sprayed coatings. A considerable amount of carbide (>60%) is decomposed during the air plasma spray (APS) process. The starting carbide does not appear to influence the extent of decarburization. All the Mo-Mo2C composite powders, with varying amounts of decarburization, show a similar percentage of carbon loss. Therefore, the balance of carbon in the coating is dependent on the starting carbon content in the powder.

Particle size plays a significant role in the extent of decarburization, as evidenced by comparison of the percent carbon loss results for the Composite 2 and Composite 2C powders. The

Table 4 Carbon discrepancy and molybdenum lattice parameter measurements

Coating	Process	Unaccounted carbon/Mo_2C		Molybdenum lattice parameter, A		Change in
		Mo_2C, wt%	Carbon, wt%	Powder	Coating	lattice parameter, %
Molybdenum	APS	...	...	3.148	3.147	0
Composite 1	APS	2	0.1	3.149	3.150	0.03
Composite 2	APS	6	0.3	3.148	3.151	0.10
Composite 2C	APS	6	0.3	3.150	3.155	0.16
Composite 3	APS	12	0.6	3.145	3.155	0.32
	Plazjet	1.7	0.1	3.145	3.148	0.09

coarser powder, with a similar starting chemistry, shows a lower carbon loss despite only small differences in particle size. This result is not surprising, because finer powder exposes a greater surface area (per unit weight of material) for the reaction.

The beneficial effect of this decarburization reaction is in reducing the oxidation of molybdenum. As can be seen from Table 3, pure molybdenum undergoes considerable oxidation during APS and displays greater than 1.0 wt% O_2 in the coating. In the case of Mo-Mo_2C, the carbon acts as a "sacrificial getter" for the oxygen, resulting in lower O_2 and oxide levels in the coatings. This event is beneficial to coating properties, as will be discussed in subsequent sections of this paper.

In an independent investigation, researchers at Nippon Steel Hardfacing thermal sprayed the Mo-55Mo_2C (Composite 3) powder using the Plazjet process (a high-velocity, high-power plasma spray process) (Ref 11). Their results indicate carbide levels greater than 20 wt% (Mo_2C) in the coating. This higher carbide retention in the Plazjet process is associated with lower particle dwell time, which results in lower exposure of the powder particle to oxidizing conditions. Nippon Steel researchers have also investigated low-pressure plasma spraying of Composite 3 powder and have found a considerably higher percentage of retained carbide in the coating. In this case, the low-pressure or inert atmosphere reduces and/or eliminates the oxidation of the carbide during plasma spraying. The hardnesses of the Plazjet and LPPS deposits are considerably higher than the APS case, a fact associated with the retained carbide in the deposits.

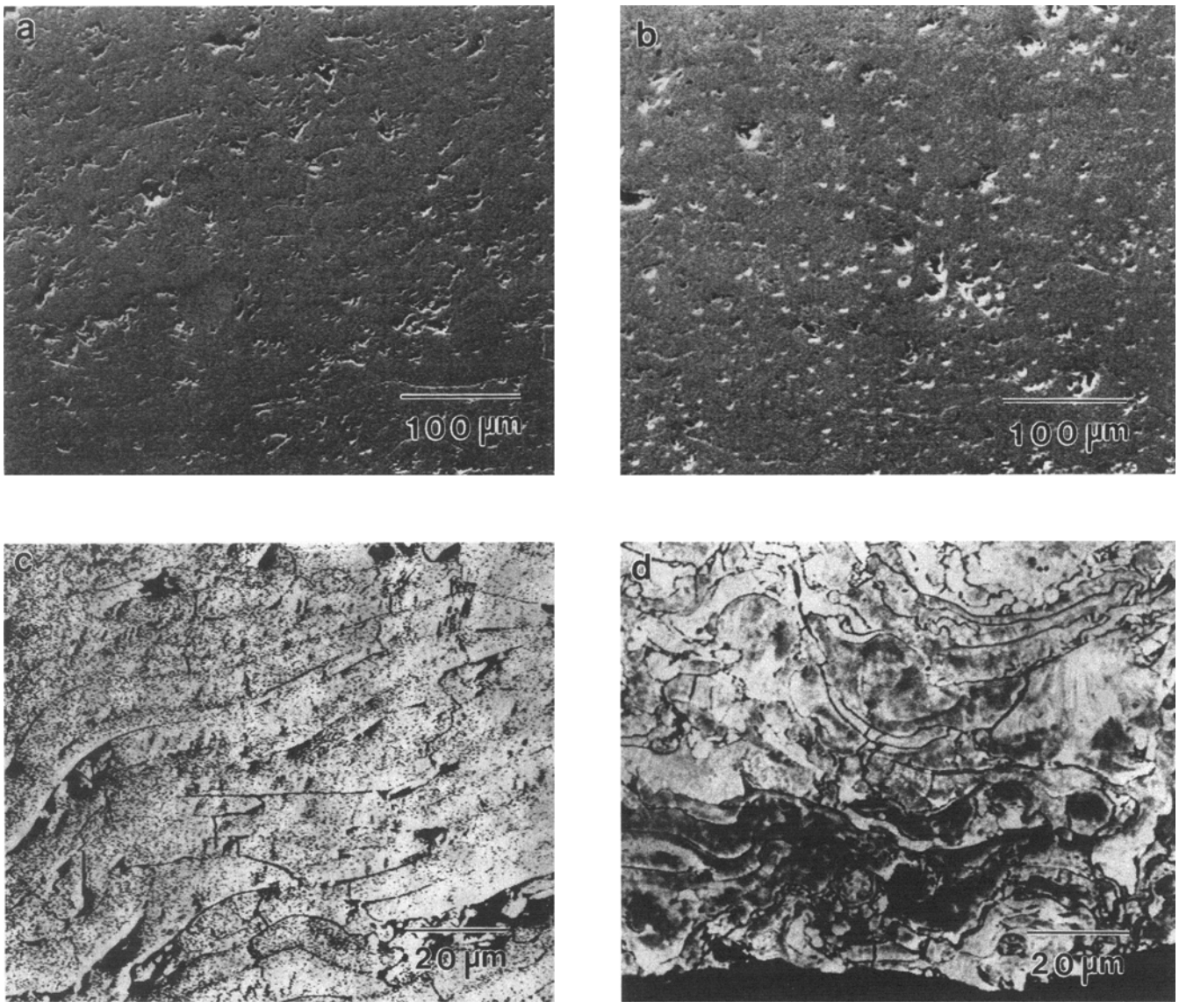

Fig. 5 Microstructures of plasma-sprayed molybdenum and Mo-Mo_2C coatings. (a) Scanning electron micrograph of plasma-sprayed molybdenum coating. (b) Scanning electron micrograph of plasma-sprayed Mo-Mo_2C coating. (c) Backscattered electron micrograph of plasma-sprayed molybdenum coating. (d) Backscattered electron micrograph of plasma-sprayed Mo-Mo_2C coating

The total carbon/carbide ratios in the powders suggest that all the carbon is accounted for, with almost no free carbon in the powder. However, the total carbon/carbide ratios in the coating do not show equivalent carbide for the total carbon present. For instance, the Composite 3 coating indicates 1.1 wt% C in the coating, which should theoretically correspond to 18 vol% Mo_2C phase. However, the coating contains only 8 vol% Mo_2C according to XRD analysis. This suggests that some excess carbon is in the free state or is supersaturated in molybdenum. Analysis of the coatings did not reveal a significant presence of free carbon, indicating that the excess carbon may be supersaturated in the molybdenum lattice.

To further evaluate the carbon supersaturation effects in molybdenum, lattice parameter measurements were utilized. Table 4 summarizes the changes in lattice parameters of the coatings with respect to the powder, in relation to the unaccounted carbon/Mo_2C numbers. It is evident that the percent change in lattice parameter increases with the increasing value of carbon discrepancy. This indicates that the carbon is supersaturated in the lattice of molybdenum. The phase diagram suggests very little solubility of carbon in molybdenum at room temperature, identified at 0.02%. The supersaturation of carbon in plasma-sprayed coatings is particularly significant in the case of Composite 3 (APS) and indicates substantial solubility of carbon (0.6 wt%) in the molybdenum lattice. Again, this result is not surprising, since solute supersaturation is commonly observed in plasma-sprayed coatings due to rapid solidification (Ref 12).

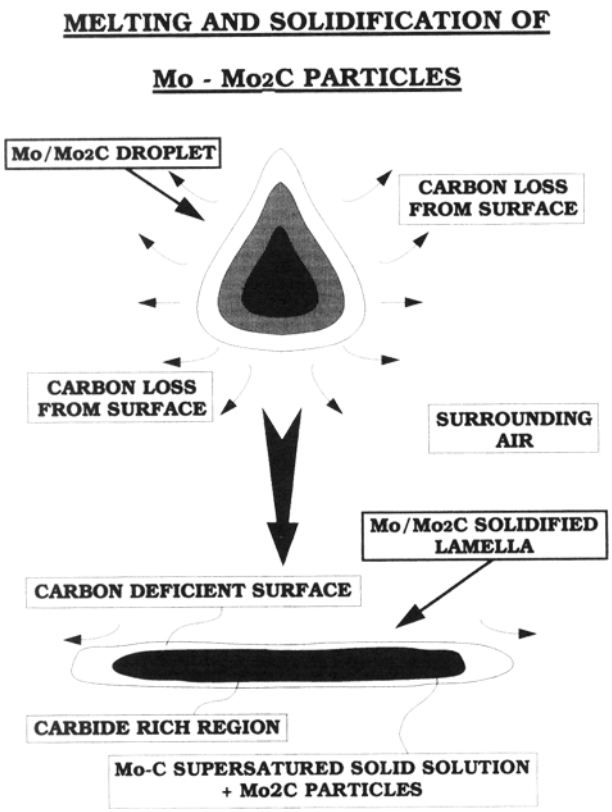

Fig. 6 Schematic depicting decarburization effects and consequent microstructural development during plasma spraying of Mo-Mo_2C composite powders

Figure 4 is a plot of percent change in lattice parameter with the percentage carbon in supersaturated solid solution (as identified in Table 4), which further illustrates the relationship between carbon supersaturation and molybdenum lattice parameter. The additional data not shown in Table 4 are for various Mo-Mo_2C coatings made using different powders and coating parameters not detailed in this paper. However, this information provides a larger set of data for developing the relationship. The plot shows a linear relationship of the lattice parameter change, with a line of best-fit regression coefficient greater than 0.9. This correlation is further evidence of the supersaturation effects of carbon in molybdenum.

3.2 *Microstructure and Hardness*

Figures 5(a) and (b) compare cross-section SEM micrographs of molybdenum and Mo-Mo_2C (Composite 2) coatings. Both coatings show limited porosity and good integrity. The presence of Mo_2C is not easily detected by SEM. However, a backscattered electron micrograph cross section of the Mo-Mo_2C coating (Fig. 5d) shows dark areas in the solidified lamellae, possibly associated with the presence of molybdenum carbide. Figure 5(c) is a backscattered electron micrograph of the molybdenum coating. The substantial presence of the Mo_2C phase in the powder and coating is confirmed by XRD analysis. An interesting aspect of Fig. 5(d) is the absence of dark Mo_2C regions on the peripheral regions of the splat. This is attributed to the decarburization reactions that occur during spraying. The decarburization effect and the consequent microstructure development are illustrated in Fig. 6. The advantage of this decarburization is the reduction or elimination of oxide scales from the surface of the lamellae, enabling a more chemically clean surface for bonding with the subsequent solidifying particle. The effect of this type of microstructure on the properties will be evident in the following section.

Table 3 lists the micro- and macrohardnesses of the various coatings in relation to the retained Mo_2C. No clear relationship is observed between hardness and the carbide content at the low carbide content levels, probably because extrinsic microstructu-

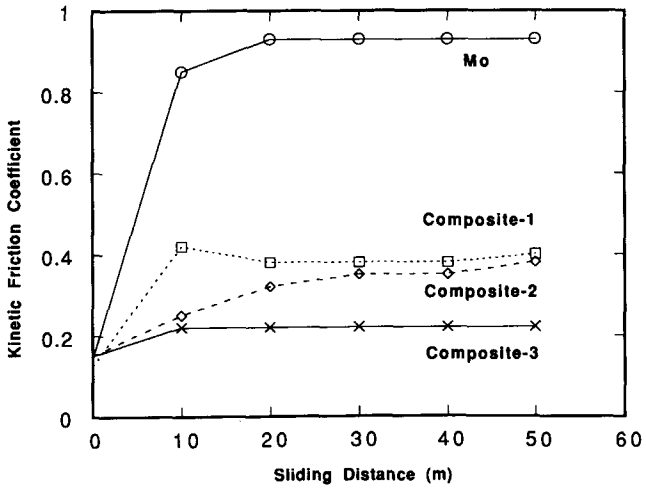

Fig. 7 Kinetic friction results obtained from ball-on-disk testing of the molybdenum and Mo-Mo_2C coatings

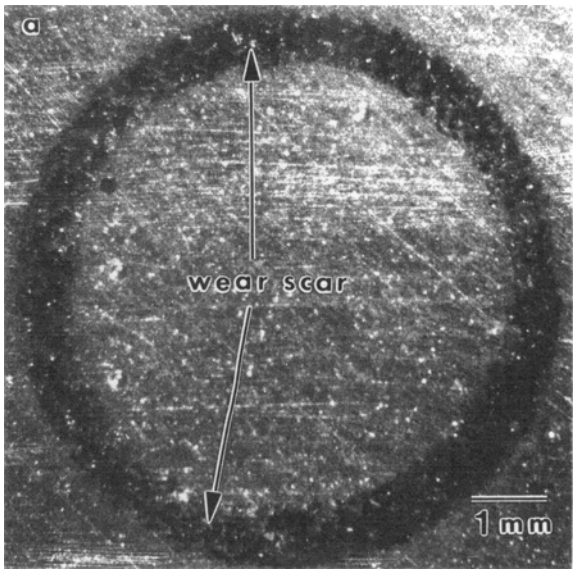

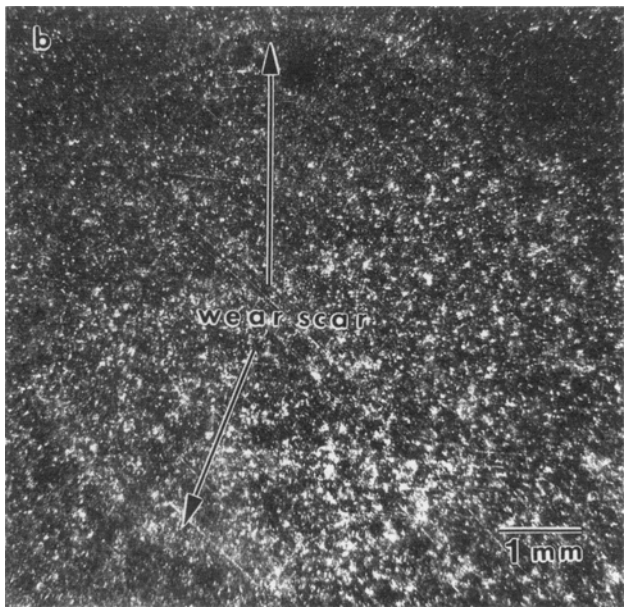

Fig. 8 Optical micrographs of wear tracks after 50 m of sliding contact during the ball-on-disk test. (a) Molybdenum coating. (b) Mo-Mo_2C coating (Composite 3)

ral factors such as porosity and the lamellar nature of the coating influence the hardness results. All the Mo-Mo_2C coatings, however, show substantially improved hardness compared to a plasma-sprayed molybdenum coating.

3.3 *Friction and Wear Characteristics*

Figure 7 compares the kinetic friction properties of the molybdenum and Mo-Mo_2C plasma-sprayed coatings obtained from the ball-on-disk test (Fig. 2). The carbide effect on this property is evident insofar that retained carbide strengthens the lamellae and thereby reduces the fracture of the individual

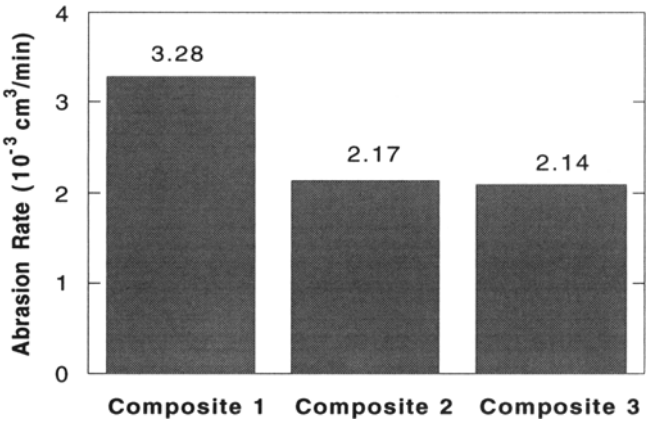

Fig. 9 Diamond abrasion test results for the molybdenum and Mo-Mo_2C coatings

splats. Additionally, the absence of MoO_2 in the Mo-Mo_2C coatings (due to sacrificial oxidation of carbon) enables a better interlamellar bond, thereby reducing the extent of delamination during continuous sliding contact.

Figure 8 compares SEM micrographs of the wear tracks on the surfaces of the molybdenum and the Mo-Mo_2C coatings after 50 m of continuous sliding contact. Considerably lower wear is observed in the Mo-Mo_2C coatings compared to the molybdenum coatings. The worn molybdenum coating indicates a larger wear track with considerable delamination and pullout from the surface. The Mo-Mo_2C coatings show a stable frictional behavior with small, localized, worn regions on the coating surface.

Figure 9 compares the results from diamond abrasion testing (Fig. 3) of the various Mo-Mo_2C coatings. Once again, the effect of Mo_2C on the abrasion properties is evident. The larger the Mo_2C content retained in the coating, the better the abrasion resistance. In this study, the abrasion properties of the molybdenum coatings have not been examined. However, Tani (Ref 13) has shown that the Mo-Mo_2C coatings exhibit substantially improved resistance to dry sand abrasion compared to plasma-sprayed molybdenum coatings.

Thus, despite only small differences in chemistry and hardness, considerable differences in friction and wear properties exist. Mo-Mo_2C coatings offer substantially improved wear properties compared to molybdenum coatings. Composition and particle size play an important role in determining the phase and microstructure, and thus the friction and wear properties, of the coatings.

4. Conclusions

Considerable decarburization occurs through an oxidation reaction during air plasma spraying of Mo-Mo_2C. The extent of decarburization is independent of the starting carbide content; however, the larger the starting carbide content in the powder, the greater the amount of carbide retained in the coating. Finer powders undergo a greater degree of decarburization than coarser powders. Low-pressure or inert-gas plasma spraying can reduce the extent of decarburization. Considerable supersaturation of carbon in molybdenum is also observed in the de-

posit. A linear relationship exists between the change in lattice parameter and the extent of carbon in solid solution.

Kinetic friction properties of molybdenum coatings are considerably improved by the controlled addition of Mo_2C to the powder. The decarburization reaction is beneficial because it reduces the extent of molybdenum oxidation during spraying. The absence of oxides improves the interlamellar bond between the layers, thereby reducing delamination effects during sliding contact. The addition of Mo_2C to molybdenum also improves the hardness of the molybdenum lamellae and thus enhances the wear resistance of the coating. Abrasive wear resistance appears to be a function of the retained carbide in the coating.

Acknowledgments

The authors thank Glenn Bancke and Professor Herbert Herman of SUNY at Stony Brook for their assistance in plasma spraying of the specimens. The authors are also grateful to Dr. David Houck of Osram Sylvania for critical review of the manuscript. Thanks also to John Luongo (GTE Labs) and Jack Vanderpool, Dave Estelle, Harry Fassett, Gail Meyers, JoAnn Cuddy, and Kathy Hammerly (all of Osram Sylvania) for their help, and to Mr. Ghislain Montavon of Stony Brook for preparing the illustrations.

References

1. J.G. Heyes and R.G.R. Sellers, High Temperature Applications of Refractory Metals, *Met. Mater.*, Feb 1992, p 86-92
2. J.A. Shields, Jr., Molybdenum and Its Alloys, Refractory Metals Forum, *Adv. Mater. Process.*, Vol 142 (No. 4), 1992, p 28-36
3. R.W. Burman, Molybdenum—A Super Superalloy, *J. Met.*, Vol 29 (No. 11), 1977, p 12-17
4. J.J. Liao, R.C. Wilcox, and R.H. Zee, Structure and Properties of the Mo-Mo_2C System, *Scr. Metall.*, Vol 24, 1990, p 1647-1652
5. B.J. Taylor and T.S. Eyre, A Review of Piston Ring and Cylinder Liner Materials, *Tribol. Int.*, Vol 12, April 1979, p 79-89
6. M.P. Overs, S.J. Harris, and R.B. Waterhouse, The Fretting Wear of Sprayed Molybdenum Coatings at Temperatures Up to 300 °C, *Wear of Materials*, K.C. Ludema, W.A. Glaeser, and S.K. Rhee, Ed., American Society of Mechanical Engineers, 1979, p 379-387
7. S. Sampath, V. Anand, and S.F. Wayne, On the Properties of Mo-based Thermal Spray Coatings for Piston Ring Applications, *Proc. 2nd Plasma Technik Symp.*, Vol 2, S.B. Sandmeier, P. Huber, H. Eschnauer, and A. Nicoll, Lucerne, Switzerland, 1991
8. D.L. Houck, D.J. Port, and J.S. Lee, "Process for Producing Composite Agglomerate of Mo-Mo_2C," U.S. Patent 4,716,019, Dec 1987
9. H. Czichos, S. Becker, and J. Lexow, Multilaboratory Tribotesting: Results from the Versailles Advanced Materials and Standards (VAMAS) Programme on Wear Test Methods, *Wear*, Vol 114, 1987, p 109-130
10. Mo-C Phase Diagram, *Constitution of Binary Alloys*, M. Hansen, Ed., 2nd ed., McGraw-Hill, 1958, p 109
11. S. Murakami, Nippon Steel Hardfacing Co. Ltd., Kitakyushu-City, Japan, private communication
12. S. Sampath, "Rapid Solidification during Plasma Spraying," Ph.D. thesis, State University of New York, Stony Brook, 1989 (University Microfilms International DA9012969)
13. K. Tani, Tocalo Co. Ltd., Kobe, Japan, private communication